AIP | The Journal of Chemical Physics

Pulsed discharge jet spectroscopy of DSiF and the equilibrium molecular structure of monofluorosilylene

Warren W. Harper, David A. Hostutler, and Dennis J. Clouthier

Citation: The Journal of Chemical Physics **106**, 4367 (1997); doi: 10.1063/1.473484
View online: http://dx.doi.org/10.1063/1.473484
View Table of Contents: http://scitation.aip.org/content/aip/journal/jcp/106/11?ver=pdfcov
Published by the AIP Publishing

Articles you may be interested in

Single vibronic level emission spectroscopic studies of the ground state energy levels and molecular structures of jet-cooled HGeBr, DGeBr, HGeI, and DGeI
J. Chem. Phys. **125**, 114301 (2006); 10.1063/1.2355496

The ground state energy levels and molecular structure of jet-cooled HGeCl and DGeCl from single vibronic level emission spectroscopy
J. Chem. Phys. **124**, 124320 (2006); 10.1063/1.2181142

The electronic spectroscopy and molecular structure of the HPCl free radical: A potential III–V semiconductor growth intermediate
J. Chem. Phys. **119**, 2037 (2003); 10.1063/1.1584032

HPO does not follow Walsh's rules! Improved molecular structures from the spectroscopy of jet-cooled HPO and DPO
J. Chem. Phys. **117**, 10604 (2002); 10.1063/1.1521130

Emission spectroscopy, harmonic vibrational frequencies, and improved ground state structures of jet-cooled monochloro- and monobromosilylene (HSiCl and HSiBr)
J. Chem. Phys. **115**, 5485 (2001); 10.1063/1.1397795

This article is copyrighted as indicated in the article. Reuse of AIP content is subject to the terms at: http://scitation.aip.org/termsconditions. Downloaded to IP: 130.70.241.163 On: Sat, 20 Dec 2014 11:39:21

Pulsed discharge jet spectroscopy of DSiF and the equilibrium molecular structure of monofluorosilylene

Warren W. Harper, David A. Hostutler, and Dennis J. Clouthier[a)]
Department of Chemistry, University of Kentucky, Lexington, Kentucky 40506-0055

(Received 15 October 1996; accepted 10 December 1996)

The jet-cooled laser induced fluorescence excitation spectrum of the $\tilde{A}\ ^1A''-\tilde{X}\ ^1A'$ band system of DSiF has been observed using the pulsed discharge jet technique. Vibrational analysis of the spectrum yielded upper state harmonic vibrational frequencies of $\omega_1=1322$, $\omega_2=444$, and $\omega_3=867$ cm^{-1}. Vibronic bands involving all of the upper state fundamentals of HSiF and DSiF have now been rotationally analyzed, allowing a determination of the excited state equilibrium structure as $r_e'(\mathrm{SiH}) = 1.526 \pm 0.014$ Å, $r_e'(\mathrm{SiF}) = 1.597 \pm 0.003$ Å, and $\theta_e'(\mathrm{HSiF}) = 115.0 \pm 0.6°$. The harmonic frequencies and centrifugal distortion constants were used to obtain harmonic force fields and average (r_z) structures for the ground and excited states. The ground state average structure was used to estimate the equilibrium structure of $r_e''(\mathrm{SiH}) = 1.528 \pm 0.005$ Å, $r_e''(\mathrm{SiF}) = 1.603 \pm 0.003$ Å, and $\theta_e''(\mathrm{HSiF}) = 96.9 \pm 0.5°$. © *1997 American Institute of Physics.* [S0021-9606(97)00311-5]

I. INTRODUCTION

Monofluorosilylene (HSiF) is a member of the silylene family of reactive intermediates. Our interest in these species stems from the role they may play in semiconductor growth processes, as described in detail elsewhere.[1–5] We have embarked on a program to study the electronic spectra of a large variety of carbenes,[6–8] silylenes,[9–11] and germylenes,[12–14] in order to determine their geometries, vibrational frequencies, rotational constants, and modes of excited state decay. Most of these species have ground states of singlet multiplicity, with the lowest excited states involving promotion of an electron from a fully occupied in-plane σ^2 orbital to an unoccupied out-of-plane $p\pi$ orbital. In most cases, only the first excited singlet state has been accessible to our laser induced fluorescence (LIF) techniques, although we have been able to obtain information about the corresponding triplet states in favorable cases.[10,12,14]

The study of the spectroscopy of HSiF has a short history. It was first observed by Ismail *et al.*[15] in infrared matrix isolation experiments in 1982, as a product of the reaction of silicon atoms with HF and DF. The authors established the ground state fundamental vibrational frequencies of HSiF and DSiF and determined a force field. A year later, Lee and Deneufville[16] recorded the LIF spectrum of HSiF by exciting the products of the reaction of silane with molecular fluorine. Analysis of the 470–390 nm vibronic band system assigned as $\tilde{A}\ ^1A''-\tilde{X}\ ^1A'$ yielded the vibrational frequencies $\nu_2'' = 860$ and $\nu_2' = 560$ cm^{-1}. The fluorescence lifetime extrapolated to zero pressure was estimated to be 185±10 ns. In 1985, two research groups reported rotational analyses of Doppler-limited LIF spectra of the 0_0^0 band of HSiF. Suzuki *et al.*[17] obtained ground and excited state rotational constants and derived molecular structures by assuming values for the Si–H bond lengths. They found that transferring the ground state force field to the excited state and varying only the bending force constant to reproduce ν_2' gave calculated centrifugal distortion constants and inertial defects which were in agreement with experiment for both states. Dixon and Wright[18] reported rotational constants in general agreement with those of Suzuki *et al.*[17] and presented a detailed simulation of the anomalous branches generated by the axis-tilting (or axis-switching)[19] mechanism. By fixing the bond angles at values obtained from *ab initio* predictions,[20] they obtained ground and excited state molecular structures.

In subsequent work, Suzuki and Hirota[21] studied the effect of magnetic fields on portions of the 0_0^0 band recorded at sub-Doppler resolution using the intermodulated fluorescence technique. They obtained the rotational g factors g_{aa}'' and g_{aa}' and discussed them in terms of the electronic Coriolis interaction between the $\tilde{X}$ and $\tilde{A}$ states. There have also been a variety of *ab initio* predictions of the properties of HSiF,[20,22–24] including values of the vibrational frequencies and geometries for the $\tilde{a}\ ^3A''$ and $\tilde{A}\ ^1A''$ excited states.[20,24]

In 1995, we reported[25] the LIF spectrum of jet-cooled HSiF, obtained by generating the radical in a chemical reaction jet through the exothermic reaction of molecular fluorine with silane, buffered by a large excess of argon. Eleven vibronic bands were identified and seven of them were rotationally analyzed. The upper state bending potential and equilibrium geometry were obtained by fitting the rovibrational energy levels of the bending (2_o^n) progression to the semirigid bender model.[26] In these calculations, the bond angle was fixed at the *ab initio* value of 114.5°, as it was found to be strongly correlated with the Si–H bond length. The resulting equilibrium bond lengths were $r_e(\mathrm{SiH})=1.548$ Å, $r_e(\mathrm{SF})=1.602$ Å. The rapid consumption of silane in our continuous flow chemical reaction jet made it prohibitively expensive to obtain spectra of DSiF from $\mathrm{SiD_4}$, so that neither the ground state r_o structure nor the excited state r_e structure could be obtained free of assumptions.

In the present work, we have devised an inexpensive method of obtaining spectra of DSiF, using the pulsed discharge jet technique and $\mathrm{DSiF_3}$ as a precursor. The previ-

---

[a)] Author to whom correspondence should be addressed.

This article is copyrighted as indicated in the article. Reuse of AIP content is subject to the terms at: http://scitation.aip.org/termsconditions. Downloaded to IP: 130.70.241.163 On: Sat, 20 Dec 2014 11:39:21

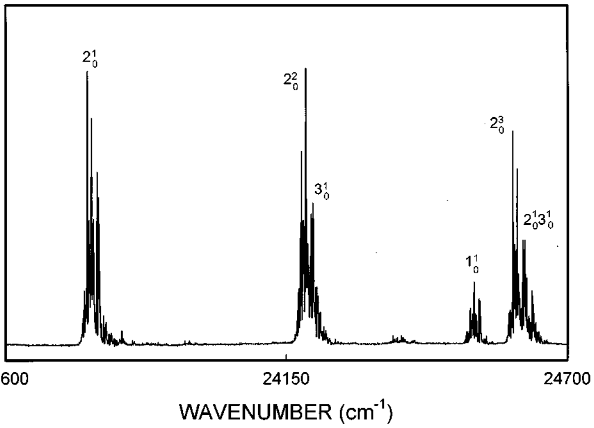

FIG. 1. A portion of the low-resolution discharge jet spectrum of HSiF showing the vibrational assignments.

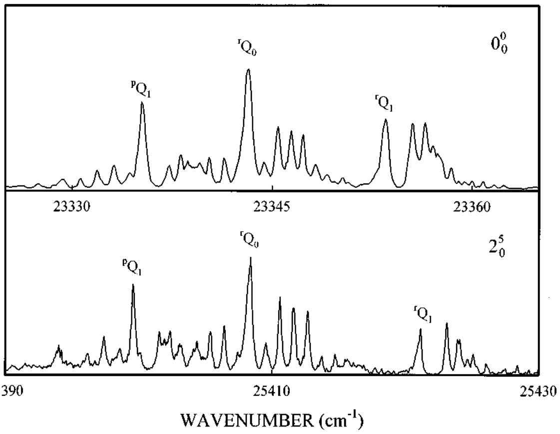

FIG. 2. Low-resolution spectra of the 0^0_0 and 2^5_0 bands of DSiF plotted on the same wavenumber scale. The 2^5_0 band shows a greater $^rQ_1 - {}^pQ_1$ separation due to a larger value of $(A-B)$ in the excited state.

ously unobserved electronic spectrum of DSiF is reported, along with new results for HSiF.

II. EXPERIMENT

The stable molecules $HSiF_3$ and $DSiF_3$ were used as precursors for the *in situ* production of HSiF and DSiF by the pulsed discharge technique. In each case, 40 Torr of the precursor was diluted with 200–400 psi of argon and the mixture stored in a cylinder equipped with a gas regulator. The gas mixture was delivered at a pressure of 40 psi to a pulsed valve (General Valve, series 9) with a 0.8 mm diam nozzle. The gas pulse expanded into a 6 mm diam flow channel drilled in a 26-mm-long Delrin cylinder attached to the end of the pulsed valve. At the appropriate time during the gas pulse, an electrical discharge was struck between two stainless steel ring electrodes mounted 1 mm apart along this channel. The discharge efficiently dissociated the precursor, producing various fragments including the monofluorosilylene, whose LIF spectrum was excited by a pulsed laser beam 30 mm beyond the end of the Delrin cylinder. The pulsed discharge jet was mounted inside a 20 in. vacuum chamber pumped by a 10 in. diffusion pump equipped with a water-cooled baffle. The typical background pressure was 2×10^{-6} Torr, with the chamber pressure rising to about 3×10^{-5} Torr during operation of the pulsed valve.

Low- ($0.5\ \mathrm{cm}^{-1}$) and medium- ($0.1\ \mathrm{cm}^{-1}$) resolution laser induced fluorescence spectra were collected using a Nd:YAG pumped pulsed dye laser (Lumonics HyperDye 300). The fluorescence was imaged onto the photocathode of a photomultiplier (EMI 9816QB), after having passed through appropriate cutoff filters to reduce scattered laser light. Etalon fringes (FSR $0.65\ \mathrm{cm}^{-1}$), along with optogalvanic lines from various argon or neon filled hollow cathode lamps, were used for calibration. High-resolution spectra ($0.04\ \mathrm{cm}^{-1}$) were recorded for selected bands using an excimer pumped dye laser equipped with an intracavity etalon (Lambda Physik FL 3002E). These spectra were calibrated to an accuracy of $\sim0.005\ \mathrm{cm}^{-1}$ using the Raman shifting and I_2 LIF technique described previously.[27] In all cases, the LIF spectra and calibration signals were recorded simultaneously on a data acquisition system developed in our laboratory.[28]

Trifluorosilane was synthesized by fluorinating trichlorosilane (Aldrich) with antimony trifluoride. $HSiCl_3$ (3–4 ml) was condensed in vacuum onto the surface of 200 gm of very dry, powdered SbF_3 in a 500 ml vessel. The vessel was sealed with a stopcock and the mixture allowed to warm up to room temperature over a period of about 30 min.[29] A rapid reaction ensued with the production of white fumes and considerable blackening of the solid phase. After the reaction appeared complete, the volatile products were vaporized into a trap cooled with liquid nitrogen, and the fraction distilling over when the trap was warmed to −98 °C was almost pure trifluorosilane. $DSiF_3$ was synthesized in the same manner using $DSiCl_3$ as the reactant. The identity and purity of the fluorosilanes were checked by gas phase infrared spectroscopy. $DSiCl_3$ was prepared by the heterogeneous reaction of DCl[30] with a mixture of 80% granular silicon and 20% $CuCl_2$ at 380 °C.[31]

III. RESULTS

A. Vibrational analysis

Monofluorosilylene is a nonlinear molecule of C_s symmetry with 3 a' normal modes of vibration labeled ν_1 (Si–H or Si–D stretch), ν_2 (bend), and ν_3 (Si–F stretch). The low symmetry of the molecule results in unrestricted vibrational quantum number changes for allowed electronic transitions.

The LIF spectrum of DSiF was recorded in the 455–380 nm region. The low wavenumber portion of the spectrum, illustrated in Fig. 1, is quite simple and bands involving all three excited state fundamentals were readily identified. At low resolution, each individual band consists of three prominent unresolved Q branches and a variety of partially resolved P and R branches, with a contour characteristic of a C-type band, as shown in Fig. 2. The $^rQ_1 - {}^pQ_1$ separations varied from band to band (see Fig. 2) and were found to give

This article is copyrighted as indicated in the article. Reuse of AIP content is subject to the terms at: http://scitation.aip.org/termsconditions. Downloaded to IP: 130.70.241.163 On: Sat, 20 Dec 2014 11:39:21

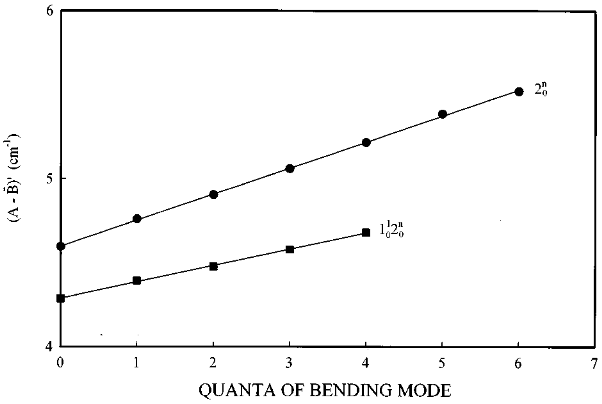

FIG. 3. Plots of the excited state $(A-\overline{B})$ values vs the number of quanta in the excited state bending mode, v_2', for the 2_0^n and $1_0^1 2_0^n$ vibrational progressions of DSiF.

near-linear plots of $(A-\overline{B})'$ vs quanta of the excited state bending mode, as shown in Fig. 3. These plots were characteristic of the particular vibrations involved, with $(A-B)'$ increasing rapidly with quanta of ν_2', decreasing very slightly with quanta of ν_3', and decreasing strongly with the addition of quanta of ν_1'. These regular trends were very useful in assigning spectra in the higher wavenumber regions where the rotational structure of the bands overlapped, as shown by the example in Fig. 4.

Although we did not find any hot bands in our previous chemical reaction jet work on HSiF, a variety of weak hot bands involving 1–3 quanta of ν_2'' were identified in the present DSiF spectra. These were assigned by matching the $(A-B)'$ values and vibrational intervals with those of the corresponding cold bands and from the observed ν_2'' value of 642 cm^{-1}, which agreed well with the infrared matrix frequency[15] of $\nu_2''=638$ cm^{-1}. The vibrational temperatures in the pulsed discharge jet technique are quite high, so that we are able to observe DSiF transitions from levels with almost 2000 cm^{-1} of vibrational energy in the ground state. Extensive hot bands have also been observed in similar work on HSiCl[32] and HSiBr.[11]

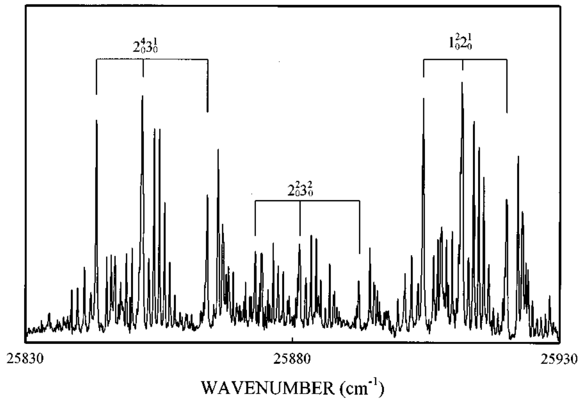

FIG. 4. A portion of the medium-resolution spectrum of DSiF in the high wavenumber region identifying Q branches and showing their vibrational assignments.

The band origins of the assigned cold bands of DSiF were estimated by adding the $K_a''=1-K_a''=0$ interval (obtained from the rotational analysis, *vide infra*) to the $^PQ_1$ branch maximum. For the hot bands, $(A-B)'$ and $(A-B)''$ values were calculated from the Q branches and then the band origins determined as before. The band origins and approximate values of $(A-B)'$ are given in Table I.

In order to obtain harmonic vibrational frequencies for a normal coordinate analysis, we first fitted the observed vibronic band origins to the vibrational anharmonicity expression:

$$\tilde{\nu}=T_{00}+\sum_{i=1}^{3}\omega_i^{0'}\nu_i'+\sum_{i=1}^{3}\sum_{j\geqslant i}^{3}x_{ij}^{0'}\nu_i'\nu_j' +\sum_{i=1}^{3}\sum_{j\geqslant i}^{3}\sum_{k\geqslant j}^{3}x_{ijk}^{0'}\nu_i'\nu_j'\nu_k'-[\omega_2^{0''}+x_{22}^{0''}(\nu_2'')^2]. \tag{1}$$

As in our previous studies of HSiBr[11] and HSiCl,[32] we found that the excited state modes are quite anharmonic and that cubic terms were necessary to fit all but the lowest energy transitions. We were particularly fortunate that in the DSiF spectrum we were able to identify the key 1_0^2 and 3_0^2 bands, so that the quadratic anharmonicity constants $x_{ii}^{0'}$ of all three modes were readily determined. The hot bands were included in the vibrational fit, but only $\omega_2^{0''}$ and $x_{22}^{0''}$ were determinable. In order to keep the set of anharmonicity constants manageable, we elected to omit four bands from the least squares analysis. In the final fit, the electronic band origin, T_{00}, was fixed at the value obtained from the analysis of the 0_0^0 band. The quality of the fit can be judged by the observed—calculated values given in Table I. Once the assigned bands were fitted to the vibrational expansion, it was then possible to calculate the upper state harmonic frequencies. The resulting constants are presented in Table III.

For the sake of consistency, we have redone the vibrational fit of the observed bands of HSiF,[25] including more constants and the more precise value of the band origin of 3_0^1 obtained in the present work (*vide infra*). The range of observed bands is much less than that of DSiF, so some assumptions about the anharmonicities were necessary. The HSiF 3_0^2 band was not observed, so $x_{33}^{0'}$ could not be fitted directly; instead we approximated it from the relationship[33]

$$\frac{x_{mn}}{x_{mn}^{i}}=\frac{\omega_m\omega_n}{\omega_m^{i}\omega_n^{i}}, \tag{2}$$

where the superscript i denotes isotopic substitution. Any error in this approximation is unlikely to have much effect on the derived harmonic frequencies, as ν_3' is not very anharmonic in the HSiX molecules we have studied. Of more concern was obtaining a good value for the har-

This article is copyrighted as indicated in the article. Reuse of AIP content is subject to the terms at: http://scitation.aip.org/termsconditions. Downloaded to IP: 130.70.241.163 On: Sat, 20 Dec 2014 11:39:21

TABLE I. Assignments, band origins, residuals from vibrational fitting, and approximate excited state $(A-\overline{B})$ values for the observed vibronic bands in the LIF spectrum of DSiF (in cm^{-1}).

Assign.	Band origin[a]	Obs.-calc.	$(A-\overline{B})'$	Assign.	Band	Obs.-calc.	$(A-\overline{B})'$
0_0^0	23338.723	0.00	4.59	$2_0^2 3_0^2$	25876.50	0.33	4.85
1_0^1	24513.046	0.30	4.29	$1_0^1 2_0^1 3_0^1$	25749.52	−11.05[b]	4.37
1_0^2	25551.22	0.00	3.89	$1_0^1 2_0^2 3_0^1$	26130.81	−13.94[b]	4.47
2_0^1	23763.525	0.20	4.76	2_1^0	22697.2	0.00	⋯
2_0^2	24182.935	0.01	4.90	2_1^1	23121.7	−0.10	⋯
2_0^3	24596.49	−0.15	5.06	2_1^2	23541.26	−0.14	4.88
2_0^4	25003.55	−0.06	5.22	2_1^3	23954.97	−0.15	5.05
2_0^5	25403.08	0.13	5.39	2_1^4	24362.10	0.01	5.23
2_0^6	25793.75	−0.02	5.52	2_1^5	24761.70	0.28	5.37
3_0^1	24193.120	−0.29	4.61	2_1^6	25152.16	−0.08	5.52
3_0^2	25038.47	0.19	4.64	$2_1^0 3_0^1$	23551.36	−0.52	⋯
$1_0^1 2_0^1$	24908.18	−0.57	4.39	$2_1^1 3_0^1$	23974.21	0.59	4.76
$1_0^1 2_0^2$	25295.67	−0.11	4.47	$2_1^2 3_0^1$	24390.30	−0.07	4.81
$1_0^1 2_0^3$	25673.66	0.71	4.58	$2_1^3 3_0^1$	24801.38	0.14	5.06
$1_0^1 2_0^4$	26039.07	−0.34	4.68	$2_1^4 3_0^1$	25205.24	−0.11	5.18
$1_0^2 2_0^1$	25907.91	−10.71[b]	3.91	$2_1^0 3_0^2$	24396.90	0.14	4.67
$2_0^1 3_0^1$	24615.74	0.59	4.75	2_2^0	22058.6	0.10	⋯
$2_0^2 3_0^1$	25031.75	−0.14	4.86	2_2^1	22483.1	0.01	⋯
$2_0^3 3_0^1$	25442.74	−0.02	5.05	2_2^2	22902.6	−0.09	⋯
$2_0^4 3_0^1$	25846.71	−0.17	5.20	2_2^3	23316.4	−0.02	⋯
$2_0^1 3_0^2$	25459.06	−0.66	4.77	2_3^2	22267.2	0.41[b,c]	⋯

[a] Band origins quoted to three decimal places are from rotational analysis and are accurate to ~0.007 cm^{-1}, those with two decimal places are estimated from medium-resolution spectra to ±0.1 cm^{-1}, and those with one decimal place are estimated from low-resolution spectra to ±1 cm^{-1}.

[b] Band not included in least squares fit.

[c] Tentative assignment of a single weak band unaccompanied by other members of the hot band progression.

monic frequency of ν_1', since it is very anharmonic in DSiF ($x_{11}^{0\prime} = -67.7$ cm^{-1}). As neither 1_0^2 nor 1_0^3 were found in the spectra of HSiF, we resorted to using the product rule expression

$$\frac{\omega_1^D \omega_2^D \omega_3^D}{\omega_1 \omega_2 \omega_3} = \left[\frac{ABC}{A^D B^D C^D}\right]^{1/2} \left[\frac{M^D}{M}\right]^{3/2} \left[\frac{m_H}{m_D}\right]^3 \tag{3}$$

to calculate the harmonic frequency. It was found that all three calculated harmonic frequencies were strongly dependent on which particular anharmonicity constants were used in the vibrational fitting, a consequence of the limited range of data available and the large anharmonicities in the excited state. Although we only used the constants necessary to properly fit the data, in the final analysis many of them were determined by single bands in the spectrum, so that their errors are likely larger than their standard errors of fit. We estimate the uncertainties in the derived harmonic frequencies of HSiF to be of the order of 10 cm^{-1}. The HSiF vibronic band origins and observed-calculated values are presented in Table II, while the resulting anharmonicity constants and harmonic frequencies are given in Table III.

TABLE II. Assignments, band origins, and residuals from vibrational fitting for the observed vibronic bands in the LIF spectrum of HSiF (in cm^{-1}).

Assign.	Band origin[a]	Obs.-calc.
0_0^0	23260.021	0.000
1_0^1	24806.970	0.000
2_0^1	23818.442	0.060
2_0^2	24366.089	−0.089
2_0^3	24901.085	0.060
2_0^4	25420.527	−0.015
3_0^1	24116.899	0.000
$1_0^1 2_0^1$	25298.7	0.000
$1_0^1 3_0^1$	25658.270	0.000
$2_0^1 3_0^1$	24671.2	0.000
$2_0^2 3_0^1$	25205.2	0.000

[a] Band origins quoted to three decimal places are from rotational analysis and are accurate to ~0.01 cm^{-1}, while those with one decimal place are accurate to ±1 cm^{-1}.

TABLE III. Vibrational constants of HSiF and DSiF (in cm^{-1}).

	HSiF	DSiF		HSiF	DSiF
$\omega_1^{0\prime}$	1546.95(9)[a]	1241.8(7)	$\omega_2^{0\prime\prime}$	⋯	642.9(3)
$\omega_2^{0\prime}$	562.9(2)	426.8(2)	$x_{22}^{0\prime\prime}$	⋯	−1.4(1)
$\omega_3^{0\prime}$	861.77(9)	859.6(4)			
$x_{11}^{0\prime}$	⋯	−67.8(4)	ω_1'	1815.6(13)	1322.4(8)
$x_{22}^{0\prime}$	−4.1(1)	−2.1(1)	ω_2'	597.1(3)	443.5(3)
$x_{33}^{0\prime}$	−4.9[b]	−4.9(2)	ω_3'	867.8(5)	867.2(5)
$x_{12}^{0\prime}$	−66.6(1)	−26.6(4)			
$x_{13}^{0\prime}$	−5.6(2)	⋯			
$x_{23}^{0\prime}$	0.8(3)	−4.1(2)			
$x_{122}^{0\prime}$	⋯	−2.0(1)			
$x_{222}^{0\prime}$	−0.40(2)	−0.15(1)			
$x_{223}^{0\prime}$	−4.9(1)	⋯			
$x_{233}^{0\prime}$	⋯	1.3(1)			

[a] The values in parentheses are one standard error in units of the last significant figure.

[b] Constant fixed in the final fit.

This article is copyrighted as indicated in the article. Reuse of AIP content is subject to the terms at: http://scitation.aip.org/termsconditions. Downloaded to IP: 130.70.241.163 On: Sat, 20 Dec 2014 11:39:21

B. Rotational analysis

Our aim in this work was to rotationally analyze the key bands in the spectra of HSiF and DSiF to obtain an excited state equilibrium (r_e) structure and an effective (r_o) ground state structure. We had previously obtained rotational constants for the 0_0^0, 2_0^1, and 1_0^1 bands of HSiF, but were unable to record the very weak 3_0^1 band at high resolution using the chemical reaction jet technique. This problem was overcome by the much better signal-to-noise ratios in the discharge jet experiments, so that we have achieved rotational analyses of the HSiF 3_0^1 band and the DSiF 0_0^0, 1_0^1, 2_0^1, and overlapping 3_0^1 and 2_0^2 bands.

During the course of the high-resolution experiments, we found that power broadening of the rotational lines in the spectra was severe, so that the laser power had to be attenuated well below 1 mJ/pulse to obtain linewidths of ~0.05 cm^{-1} full width at half-maximum (FWHM). A typical example of the DSiF spectra is the 1_0^1 band, illustrated in Fig. 5, which exhibits almost completely resolved $^rQ_0$ and $^rQ_1$ branches and $^rR_1$ asymmetry splittings.

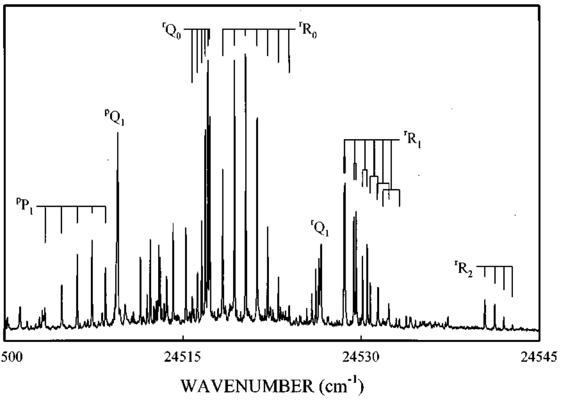

FIG. 5. The high-resolution spectrum of the 1_0^1 band of DSiF showing some of the rotational assignments.

The rotational analyses of the spectra were similar to that described previously for HSiF.[25] The electronic transition moment is oriented out of the molecular plane, giving rise to C-type bands with the selection rules $\Delta K_a = \pm 1$, $\Delta K_c = 0, \pm 2$. Although weak axis-tilting lines were found in the spectra, they were not used in the least squares fitting. Independent values of B and C were obtained from assignments of the asymmetry split $K_a' = 2 - K_a'' = 1$ and $K_a' = 1 - K_a'' = 2$ subbands. Once the assignments were completed, the rotational constants were determined by a least squares fitting of the observed transition frequencies to Watson's A reduction of the asymmetric top rotational Hamiltonian in the I^r representation.[34] For the 1_0^1 band of DSiF, the constants of both states were varied, with Δ_K'' fixed at the HSiF ground state value of 4.8×10^{-4} cm^{-1}. The other DSiF bands were fitted with the ground state constants fixed at those obtained from the 1_0^1 band. The 3_0^1 band of HSiF was fitted with the ground state constants and the excited state

TABLE IV. Rotational line frequencies (cm^{-1}) and assignments for the 1_0^1 band of DSiF.

$K_a'=1-K_a''=0$ subband				$K_a'=0-K_a''=1$ subband			
J'	$^rR_0$	$^rQ_0$	$^rP_0$	J'	$^pR_1$	$^pQ_1$	$^pP_1$
1	24518.332(−5)[a]	24517.252(−2)	24515.245(−2)	0			24508.495(−5)
2	24519.326(4)	24517.098(−5)	24514.175(1)	1		*24509.530(−19)	24507.353(1)
3	24520.278(−5)	24516.873(−5)	24513.084(2)	2	24511.440(−2)	*24509.530(13)	24506.118(−2)
4	24521.231(7)	24516.576(−6)	24511.988(11)	3	*24512.270(15)	*24509.417(−51)	24504.806(1)
5	24522.137(−9)	24516.223(4)	24510.862(−1)	4	24512.984(4)	*24509.417(16)	24503.412(7)
6	24523.049(−4)	24515.787(−5)		5	24513.632(13)	24509.320(3)	24501.915(−6)
7	24523.945(−3)			6	24514.175(5)	24509.217(5)	
8	24524.836(−1)			7		24509.084(−3)	

$K_a'=2-K_a''=1$ subband				$K_a'=1-K_a''=2$ subband		$K_a'=3-K_a''=2$ subband	
J'	$^rR_1$	$^rQ_1$	J'	$^pQ_2$	$^pP_2$	J'	$^rR_2$
2	24528.562(−4)	24526.445(9)	1		24501.315(−9)	3	24540.394(−2)
	24528.634(0)	24526.640(0)			24501.269(−4)	4	24541.227(1)
3	24529.382(0)	24526.189(3)	2	24503.181(1)	24500.243(0)	5	24541.999(−7)
	24529.577(−6)	24526.599(4)		24503.340(0)	24500.089(0)	6	24542.725(−8)
4	24530.131(13)	24525.851(−3)	3	24502.951(3)	24499.135(2)		
	24530.520(4)	*24526.599(60)		24503.274(4)	24498.827(−4)		
5	24530.782(8)	24525.436(−3)	4	24502.633(0)			
	24531.433(−2)	*24526.445(−27)		24503.181(5)			
6	24531.351(−5)	24524.944(1)	5	24502.233(0)			
	24532.341(2)			24503.058(−2)			
7	24531.859(−9)						
	24533.229(0)						

[a] The numbers in parentheses are observed minus calculated values in units of 10^{-3} cm^{-1}. An asterisk denotes a blended line not used in the least squares fit. In cases where the asymmetry doubling is resolved, the transition with even parity ($J + K_a + K_c$) in the lower state is listed first.

This article is copyrighted as indicated in the article. Reuse of AIP content is subject to the terms at: http://scitation.aip.org/termsconditions. Downloaded to IP: 130.70.241.163 On: Sat, 20 Dec 2014 11:39:21

TABLE V. Excited state rotational constants and band origins for various vibronic bands of the $\tilde{A}\ ^1A'' \leftarrow \tilde{X}\,^1A'$ system of DSiF and the 3^1_0 band of HSiF (in cm^{-1}).

Band	$A^{a,b}$	B	C	$10^3\ \Delta_K$	T_0	σ^c
0^0_0	$5.0856_5(35)$	$0.51801_3(51)$	$0.46693_3(87)$	$0.81_1(36)$	23338.723(6)	0.006
2^1_0	$5.2517_2(38)$	$0.52105_1(86)$	$0.46518_1(98)$	$1.99_7(42)$	23763.525(7)	0.008
2^2_0	$5.3983_2(38)$	$0.52268_2(55)$	$0.46541_8(53)$	$2.74_4(40)$	24182.935(7)	0.006
3^1_0	$5.0969_8(32)$	$0.51428_8(60)$	$0.46418_6(71)$	$1.05_6(34)$	24193.120(6)	0.006
1^1_0	$4.7755_5(23)$	$0.51692_4(34)$	$0.46405_4(44)$	$1.11_4(26)$	24513.046(5)	0.005
3^1_0(HSiF)[d]	$9.2959_8(18)$	$0.54410_7(44)$	$0.51329_0(65)$	3.876 015	24116.899(6)	0.007

[a] The numbers in parentheses are 3σ error limits and are right justified to the last digit on the line; sufficient additional digits are quoted to reproduce the original data to full accuracy.

[b] The ground state constants used in the analysis of the DSiF bands, obtained from fitting the upper and lower states of the 1^1_0 band are $A=3.9972_9(13)$, $B=0.54924_2(40)$, $C=0.48146_1(42)$ with Δ_K fixed at the HSiF value of 4.8×10^{-4}.

[c] Overall standard deviation of fit.

[d] The upper state centrifugal distortion constants of HSiF were fixed at the following values from the analysis of the 0^0_0 band of Ref. 20: $\Delta_K=3.876\,015\times10^{-3}$, $\Delta_{JK}=3.635\,849\times10^{-5}$, $\Delta_J=8.005\,538\times10^{-7}$, $\delta_K=3.735\,918\times10^{-5}$, $\delta_J=5.537\,164\times10^{-8}$. The lower state rotational and quartic centrifugal distortion constants were fixed at the values given in Ref. 20.

centrifugal distortion constants fixed at those obtained by Suzuki *et al.*[17] for the 0^0_0 band. An example of the quality of the fit and the range of assignments is given in Table IV. The resulting molecular constants are summarized in Table V. All of the bands fit very well, with no evidence of heterogeneous perturbations or systematic calibration errors.

IV. DISCUSSION

A. Harmonic force field

In the present work, we have been able to calculate the excited state harmonic vibrational frequencies of both HSiF and DSiF, as given in Table III. It is unfortunate that the

TABLE VI. The harmonic force field of HSiF.

Fitted data (cm^{-1})								
	$\tilde{X}$				$\tilde{A}$			
	HSiF		DSiF		HSiF		DSiF	
	Obs.	Calc.	Obs.	Calc.	Obs.	Calc.	Obs.	Calc.
ω_1	1913.1	1977.3	1387.4	1423.3	1815.6	1836.3	1322.4	1321.2
ω_2	859.0	861.0	638.4	636.0	597.1	590.2	443.5	442.4
ω_3	833.7	834.1	833.4	836.0	867.8	870.8	867.2	866.9
Δ_J	8.5×10^{-7}	9.0×10^{-7}			8×10^{-7}	8×10^{-7}		
Δ_{JK}	2.25×10^{-5}	2.25×10^{-5}			3.64×10^{-5}	3.63×10^{-5}		
Δ_K	4.80×10^{-4}	4.81×10^{-4}			3.88×10^{-3}	3.87×10^{-3}		
δ_J	5.7×10^{-8}	6.4×10^{-8}			5.5×10^{-8}	4.9×10^{-8}		
δ_K	1.4×10^{-5}	1.4×10^{-5}			3.7×10^{-5}	2.3×10^{-5}		

Internal coordinates
$R_1=\Delta r(\mathrm{Si{-}H})$
$R_2=\Delta\theta(\mathrm{HSiF})$
$R_3=\Delta r(\mathrm{Si{-}F})$

Harmonic force constants

	$\tilde{X}$	$\tilde{A}$
f_{11} (aJ Å^{-2})	2.24(2)	1.92(1)
f_{22} (aJ rad^{-2})	0.922(9)	0.46(2)
f_{33} (aJ Å^{-2})	4.76(6)	5.12(6)
f_{12} (aJ Å^{-1} rad^{-1})	⋯	0.26(2)
f_{13} (aJ Å^{-2})	0.21(5)	⋯
f_{23} (aJ Å^{-1} rad^{-1})	0.27(4)	0.17(2)

This article is copyrighted as indicated in the article. Reuse of AIP content is subject to the terms at: http://scitation.aip.org/termsconditions. Downloaded to IP: 130.70.241.163 On: Sat, 20 Dec 2014 11:39:21

TABLE VII. Structural parameters of HSiF.

	Electronic state								
	$\tilde{X}\ ^1A'$				$\tilde{A}\ ^1A''$				
	r_o	r_z	r_e^z	*Ab initio*[c]	r_o	r_e	r_z	r_e^z	*Ab initio*[d]
r (SiF) Å	1.606(1)[a]	1.608(1)[a]	1.603(3)[b]	1.615	1.602(1)[a]	1.597(3)[a]	1.603(1)[a]	1.598(3)[b]	1.617
r (SiH) Å	1.548(3)	1.542(2)	1.528(5)	1.528	1.557(1)	1.526(14)	1.555(4)	1.536(5)	1.535
θ (HSiF) °	97.0(6)	96.9(4)	96.9(5)	96.8	114.4(3)	115.0(6)	114.3(2)	114.3(5)	114.9

[a] Numbers in parentheses are one standard error in units of the last significant figures.
[b] Numbers in parentheses are estimated uncertainties in units of the last significant figures.
[c] CCSD TZ($2df$,$2pd$) results of Ref. 24.
[d] MRCI TZ($2df$,$2pd$) results of Ref. 24.

range of HSiF vibronic bands is so restricted, as this severely limits the accuracy of our derived frequencies. However, the availability of a good set of centrifugal distortion constants for the ground and excited states, from the gas phase analysis of the 0_0^0 band,[17] makes it possible to calculate reasonable harmonic force fields. The normal coordinate problem was set up in internal coordinates and the force constants were refined using the program of Hedberg and Mills.[35] The excited state harmonic frequencies were used with an estimated uncertainty of 10 cm^{-1} for HSiF and 2 cm^{-1} for DSiF, along with the centrifugal distortion constants of HSiF[17] and their statistical uncertainties. Our r_e structure (*vide infra*) was used in the calculation. For the ground state, the matrix infrared frequencies of Ref. 15 were used, with estimated errors of 30 cm^{-1} for the very anharmonic Si–H and Si–D stretches and 2 cm^{-1} for the other frequencies. The ground state gas phase centrifugal distortion constants of HSiF were also included in the fit with their statistical uncertainties.[15] The ground state structure used as input for the normal coordinate analysis was the r_e^z structure given in Table VII.

The results of the force field calculations are summarized in Table VI. Only five of the six force constants could be determined in each state. In the ground state, ω_2 and ω_3 fit well, while ω_1 was predicted to be substantially higher than observed in the matrix, consistent with the large anharmonicities expected for the Si–H/Si–D stretching vibrations. In the excited state, the DSiF harmonic frequencies fit very well, but those of HSiF show substantial errors, consonant with our expectations based on the lack of data for the higher vibronic bands of HSiF. Different weighting schemes for the vibrational frequencies did not have a substantial effect on the resulting force constants. The centrifugal distortion constants, which are the primary data determining the force fields in both states, typically fit within the limits of experimental error.

The HSiF ground state Si–H (2.24 aJ Å^{-2}) and Si–F (4.76 aJ Å^{-2}) stretching force constants are similar to those of SiH_2 (2.20 aJ Å^{-2})[36] and SiF_2 (5.03 aJ Å^{-2}),[37] but smaller than the corresponding silane force constants[38] which are 2.84 aJ Å^{-2} for SiH_4 and 7.18 aJ Å^{-2} for SiF_4. The force constants show the expected trends on excitation, consistent with the changes in the vibrational frequencies and the geometry (*vide infra*).

B. Molecular structure

Several molecular structures were calculated using a variety of different approaches. First, we used the ground and excited state rotational constants to calculate effective or r_o structures. Our initial attempts at least squares fitting of the rotational constants resulted in a very high degree of correlation between the Si–H bond length and the HSiF angle (correlation coefficient greater than 0.99); fitting planar moments decreased the correlations substantially and gave a more satisfactory fit. Consequently, for the r_o-, r_z-, and r_e-based structures, the three structural parameters were fitted to the principal planar moments, P_A and P_B, calculated from the rotational constants of HSiF and DSiF. Since the planarity condition constrains the third planar moment to zero, the experimental values of P_C were omitted from the fit. For the r_o structures, a shrinkage of the Si–D bond of 0.003 Å (Laurie correction) was included in the analysis.

The availability of rotational constants for excited state levels involving one quantum of each of the fundamentals of HSiF and DSiF made it possible to calculate an equilibrium structure. Using the data in Table V and our previous HSiF rotational constants from Ref. 25, we calculate the equilibrium rotational constants (in cm^{-1}) to be:

	HSiF	DSiF
A_e	$=9.61491\pm0.00165$	5.15200 ± 0.00178
B_e	$=0.55034\pm0.00047$	0.51890 ± 0.00029
C_e	$=0.52094\pm0.00047$	0.47062 ± 0.00044

The inertial defect $\Delta=I_C^e-I_A^e-I_B^e$ for HSiF is effectively zero ($\Delta=-0.025\pm0.039$ amu Å^2) and attests to the quality of the rotational constants. For DSiF, the inertial defect is 0.061 ± 0.038 amu Å^2, slightly larger than zero. This effect is due to the interaction of the DSiF excited state 3^1 and 2^2 levels, whose perturbed positions are only 10.2 cm^{-1} apart. Due to the low symmetry of the molecule, these levels can interact by both Fermi and c-axis Coriolis mechanisms. We have attempted to correct the rotational constants of the 3^1 level by a variety of schemes, but these did not improve the inertial defect. Unfortunately, in the excited states of molecules of this type, the A rotational constants do not scale linearly with the number of quanta of the bending mode, so that the usual linear expansion of the vibrational dependence

This article is copyrighted as indicated in the article. Reuse of AIP content is subject to the terms at: http://scitation.aip.org/termsconditions. Downloaded to IP: 130.70.241.163 On: Sat, 20 Dec 2014 11:39:21

of the rotational constant is not reliable beyond $v_2' = 1$, making corrections for Fermi resonances difficult.

The r_o and r_e structures, obtained by fitting the planar moments, are given in Table VII. Comparison of the r_o structures suggests that electronic excitation produces a slight decrease in the Si–F bond length, a slight increase in the Si–H bond length, and a large increase in the HSiF bond angle. As expected, the excited state r_e structure has shorter bond lengths than the r_o structure, although the error limits on the Si–H equilibrium bond length are disappointingly large.

We have also used the results of our normal coordinate analysis to obtain average (r_z) structures for the ground and excited states. The harmonic contributions to the α constants, obtained from the harmonic force field, were added to the $v=0$ effective rotational constants (Table V) and the resulting constants (transformed to planar moments) were fitted to the geometric parameters. The contraction in the Si–H bond length on deuterium substitution was calculated using the equation[39–41]

$$\delta r_z = \frac{3}{2}\, a\, \delta\langle u^2\rangle - \delta K \tag{4}$$

with the zero-point mean-square amplitude of the bond, $\langle u^2\rangle$, and its perpendicular amplitude correction, K, obtained from the force field. The Morse anharmonicity parameters a, were calculated from the relation[42]

$$a = \frac{2}{3}\, \pi\omega_e \sqrt{\frac{c\mu}{2hB_e^3}} \left(\frac{\alpha_e + 6B_e^2}{\omega_e}\right) \tag{5}$$

using spectroscopic data from the SiH[43] and SiF[44] diatomic molecules. Finally, estimated equilibrium bond lengths (we have termed this the r_e^z structure) were obtained from the r_z structure using the formula[39–41]

$$r_e^z = r_z - \frac{3}{2}\, a\langle u^2\rangle + K. \tag{6}$$

The bond angles were assumed to be the same in the r_z and r_e^z structures and the results are given in Table VII.

The excited state r_e and r_e^z structures compare quite favorably, indicating that the r_e^z structure in the ground state is probably fairly close to the equilibrium structure. Our best estimates of the equilibrium molecular geometries in the ground and excited states are therefore the r_e^z and r_e structures, respectively, as given in Table VII. The ground state bond lengths of $r(\mathrm{SiF})=1.603(3)$ and $r(\mathrm{SiH})=1.528(5)$ are comparable to the equilibrium bond lengths of SiF (1.6011 Å)[44] and SiH (1.5201 Å).[43] The ground state bond angle of 96.9(5)° is very nearly equal to the average (96.43°) of the equilibrium ground state bond angles of difluorosilylene[45] (100.77°) and silylene[36] (92.08°). Electronic excitation decreases the $r(\mathrm{SiF})$ bond length by 0.006 ± 0.004 Å, in accord with the experimental and force field results which show $\omega_3' > \omega_3''$. The error bars on the excited state $r(\mathrm{SiH})$ bond length do not allow a direct determination of the effect electronic excitation has on the Si–H bond length, but the *ab initio* predictions and the decrease in ω_1 and f_{11} suggest a slight elongation.

In this work, the ground and excited state molecular structures of HSiF have been obtained free of assumptions for the first time. In comparing the r_e' and $r_e^{z\prime\prime}$ structures to the high quality *ab initio* predictions in Table VII, we note that the agreement is within the uncertainties of the experimental results, except for the Si–F bond lengths which are consistently overestimated by theory. The present excited state equilibrium bond lengths are also in general agreement with those previously derived from our semirigid bender fit of only HSiF rovibronic energy levels, in which the excited state bond angle was assumed to be 114.5°.

ACKNOWLEDGMENTS

Many helpful discussions with Dr. Roger Grev are gratefully acknowledged and we thank him for providing us with his *ab initio* predictions prior to their publication. We are greatly indebted to Professor H. D. Rudolph for providing us with copies of his structure programs and much advice on their implementation. This research was supported by the National Science Foundation. D.A.H. is an NSF summer Research Experiences for Undergraduates (REU) Student.

[1] J. M. Jasinski, B. S. Meterson, and B. A. Scott, Ann. Rev. Phys. Chem. **38**, 109 (1987).
[2] M. J. Vasile and F. A. Stevie, J. Appl. Phys. **53**, 3799 (1982).
[3] Y. Matsumi, S. Toyoda, T. Hayashi, M. Miyamura, H. Yoshikawa, and S. Komiya, J. App. Phys. **60**, 4102 (1986).
[4] S. Vanhaelemeersch, J. Van Hoeymissen, D. Vermeylen, and J. Peeters, J. Appl. Phys. **70**, 3892 (1991).
[5] G. H. Kruppa, S. K. Shin, and J. L. Beauchamp, J. Phys. Chem. **94**, 327 (1990).
[6] D. J. Clouthier and J. Karolczak, J. Chem. Phys. **94**, 1 (1991).
[7] J. Karolczak, D. L. Joo, and D. J. Clouthier, J. Chem. Phys. **99**, 1447 (1993).
[8] J. Karolczak and D. J. Clouthier (unpublished).
[9] J. Karolczak and D. J. Clouthier, Chem. Phys. Lett. **201**, 409 (1993).
[10] J. Karolczak, R. H. Judge, and D. J. Clouthier, J. Am. Chem. Soc. **117**, 9523 (1995).
[11] H. Harjanto, W. W. Harper, and D. J. Clouthier, J. Chem. Phys. **105**, 10189 (1996).
[12] J. Karolczak, Q. Zhuo, D. J. Clouthier, W. M. Davis, and J. D. Goddard, J. Chem. Phys. **98**, 60 (1993).
[13] J. Karolczak, R. S. Grev, and D. J. Clouthier, J. Chem. Phys. **101**, 891 (1994).
[14] J. Karolczak, W. W. Harper, R. S. Grev, and D. J. Clouthier, J. Chem. Phys. **103**, 2839 (1995).
[15] Z. K. Ismail, L. Fredin, R. H. Hauge, and J. L. Margrave, J. Chem. Phys. **77**, 1626 (1982).
[16] H. U. Lee and J. P. Deneufville, Chem. Phys. Lett. **99**, 394 (1983).
[17] T. Suzuki, K. Hakuta, S. Saito, and E. Hirota, J. Chem. Phys. **82**, 3580 (1985).
[18] R. N. Dixon and N. G. Wright, Chem. Phys. Lett. **117**, 280 (1985).
[19] J. T. Hougen and J. K. G. Watson, Can. J. Phys. **43**, 298 (1965).
[20] M. E. Colvin, R. S. Grev, H. F. Schaefer, and J. Bicerano, Chem. Phys. Lett. **99**, 399 (1983).
[21] T. Suzuki and E. Hirota, J. Chem. Phys. **85**, 5541 (1986).
[22] B. T. Luke, J. A. Pople, M. B. Krogh-Jespersen, Y. Apeloig, M. Karni, J. Chandrasekhar, and P. v. R. Schleyer, J. Am. Chem. Soc. **108**, 270 (1986).
[23] S. K. Shin, W. A. Goddard, and J. L. Beauchamp, J. Chem. Phys. **93**, 4986 (1990).
[24] K. J. Gregory and R. S. Grev (unpublished).
[25] W. W. Harper, J. Karolczak, D. J. Clouthier, and S. C. Ross, J. Chem. Phys. **103**, 883 (1995).

This article is copyrighted as indicated in the article. Reuse of AIP content is subject to the terms at: http://scitation.aip.org/termsconditions. Downloaded to IP: 130.70.241.163 On: Sat, 20 Dec 2014 11:39:21

[26] P. R. Bunker and B. M. Landsberg, J. Mol. Spectrosc. **67**, 374 (1977).
[27] D. J. Clouthier and J. Karolczak, Rev. Sci. Instrum. **61**, 1607 (1990).
[28] M. L. Rutherford, D. J. Clouthier, and F. J. Holler, Appl. Spectroc. **43**, 532 (1989).
[29] H. J. Emeleus and A. G. Maddock, J. Chem. Soc., 293 (1944).
[30] H. C. Brown and C. Groot, J. Am. Chem. Soc. **64**, 2223 (1942).
[31] G. Brauer, Handbook of Preparative Inorganic Chemistry, **I**, 691 (1963).
[32] W. W. Harper and D. J. Clouthier (unpublished).
[33] G. Herzberg, *Molecular Spectra and Molecular Structure II. Infrared and Raman Spectra of Polyatomic Molecules* (Van Nostrand, New York, 1945), p. 229.
[34] J. K. G. Watson, in *Vibrational Spectra and Structure, a Series of Advances*, edited by J. R. Durig (Elsevier, New York, 1977), Vol. 6, pp. 1–89.
[35] L. Hedberg and I. M. Mills, J. Mol. Spectrosc. **160**, 117 (1993).
[36] C. Yamada, H. Kanamori, E. Hirota, N. Nishiwaki, N. Itabashi, K. Kato, and T. Goto, J. Chem. Phys. **91**, 4582 (1989).
[37] H. Shoji, T. Tanaka, and E. Hirota, J. Mol. Spectrosc. **47**, 268 (1973).
[38] T. Shimanouchi, I. Nakagawa, J. Hiraishi, and M. Ishii, J. Mol. Spectrosc. **19**, 78 (1966).
[39] K. Kuchitsu, J. Chem. Phys. **49**, 4456 (1968).
[40] K. Kuchitsu, T. Fukuyama, and Y. Morino, J. Mol. Struct. **1**, 463 (1968).
[41] K. Kuchitsu, T. Fukuyama, and Y. Morino, J. Mol. Struct. **4**, 41 (1969).
[42] K. Kuchitsu and Y. Morino, Bull. Chem. Soc. Jpn. **38**, 805 (1965).
[43] G. Herzberg, A. Lagerqvist, and B. J. McKenzie, Can. J. Phys. **47**, 1889 (1969).
[44] R. W. Martin and A. J. Merer, Can. J. Phys. **51**, 634 (1973).
[45] H. Shoji, T. Tanaka, and E. Hirota, J. Mol. Spectrosc. **47**, 268 (1973).

This article is copyrighted as indicated in the article. Reuse of AIP content is subject to the terms at: http://scitation.aip.org/termsconditions. Downloaded to IP: 130.70.241.163 On: Sat, 20 Dec 2014 11:39:21